MICHIGAN STATE UNIVERSITY

CYCLOTRON LABORATORY

NUCLEAR COLLISIONS AT INTERMEDIATE ENERGY

David K. Scott

Presented at the International Conference on Nuclear Physics, August 24-30, 1980, at Berkeley, California

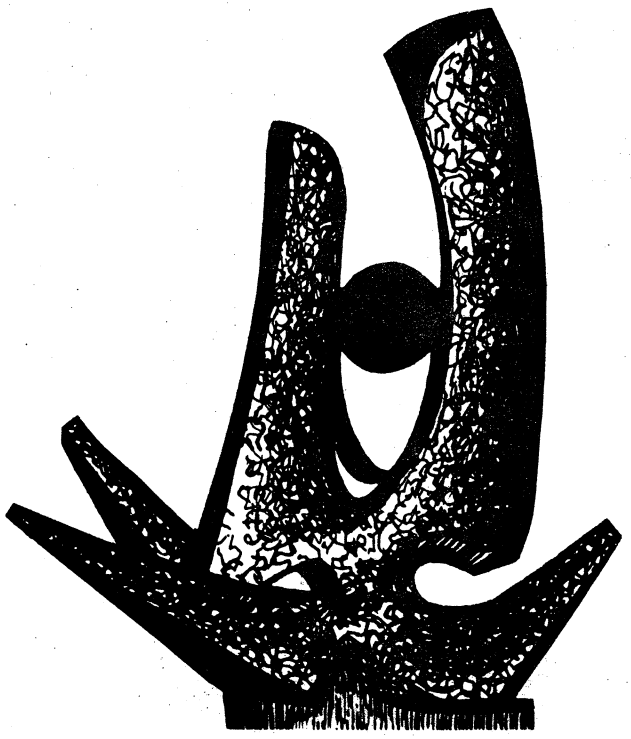

August, 1980

MSUCL-337

MSUCL-337
August 1980

NUCLEAR COLLISIONS AT INTERMEDIATE ENERGY

David K. Scott

National Superconducting Cyclotron Laboratory
and
Departments of Physics and Chemistry
Michigan State University
East Lansing, Michigan 48824, U.S.A.

Abstract: Intermediate energy nuclear collisions in the energy region from approximately 10 to 200 MeV/u are discussed. Their importance in providing conceptual links between low and high energy processes is emphasised. The production of spectator fragments, of a participant or localised hot zone and of composite light particles by coalescence can already be discerned at 15 MeV/u. The transition from fusion in central collisions to explosive reactions also appears to take place at fairly low energies. Intermediate energy studies may be useful in relating low energy microscopic theories of TDHF, direct and multistep reactions to the macroscopic approaches such as nuclear hydrodynamics.

1. Introduction

Largely as a result of developments in accelerator technology, the study of nuclear collisions has been focused on two decades of incident energy: from 1 to 10 MeV/u by the numerous electrostatic and cyclotron accelerators throughout the world, and from 200 to 2000 MeV/u by modifications to existing synchrotrons. It has, however, become clear that the intervening decade from approximately 10 to 100 MeV/u contains important transitional features, a fact emphasised by the intense activity in the construction of intermediate energy accelerators. Some of the recently completed and proposed machines with their approximate energy domains are shown in Fig. 1, along with the characteristic physics expected. In the transitional region, the collision speed surpasses both the sound velocity and the intrinsic Fermi velocity. Instead of a mean field description, one may find that the mean free path of nucleons becomes short before nuclei lose their cohesiveness; hydrodynamic features may therefore come into play. On the other hand the energy is not so high

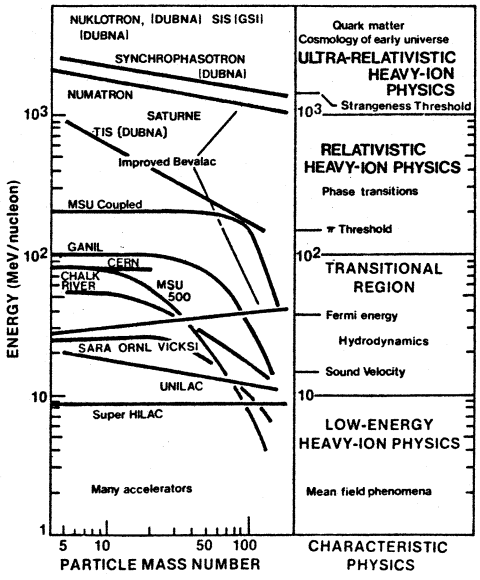

FIG. 1. The energy regions and possible characteristic physics covered by recently constructed and proposed heavy-ion accelerators. In cases where several machines cover similar ranges, only one representative line is shown.

that the reaction processes could be dominated by nucleon-nucleon collisions. The region forms a bridge, with one side planted firmly in traditional heavy-ion physics, but with the other side leading into the precursors of high energy phenohena. This paper deals with the first insights gleaned from pushing existing low and high energy machines into the intermediate domain.

2. General features of nuclear collisions

A graphic illustration of the significance of intermediate energies comes from streamer chamber and emulsion photographs. The bottom left-hand frame in Fig. 2 illustrates the typical outcome of a low energy heavy-ion reaction:[1]) a carbon beam of 25 MeV/u is incident from the left and collides with ^{20}Ne, leading to three particles in the final state. At the opposite extreme is the collision of Argon at 1800 MeV/u in an emulsion,[2]) in which both nuclei are completely shattered. But these explosive events can also take place at 25 MeV/u as illustrated at the bottom right, again for ^{12}C + ^{20}Ne at 25 MeV/u, and they are certainly well developed by 91 MeV/u[3]) (see the example for ^{12}C in an emulsion, top right). The occurrence of these high multiplicity events at energies of 25 and 91 MeV/u is one of the most compelling reasons for the study of intermediate energy heavy-ion collisions. From the debris of the explosive events at relativistic energies one hopes to reconstruct the history of the early, possibly exotic, prevailing conditions. Although exotic processes due to phase transitions are perhaps less likely at intermediate energies, it seems that the basic underlying processes leading to these violent events are already present.

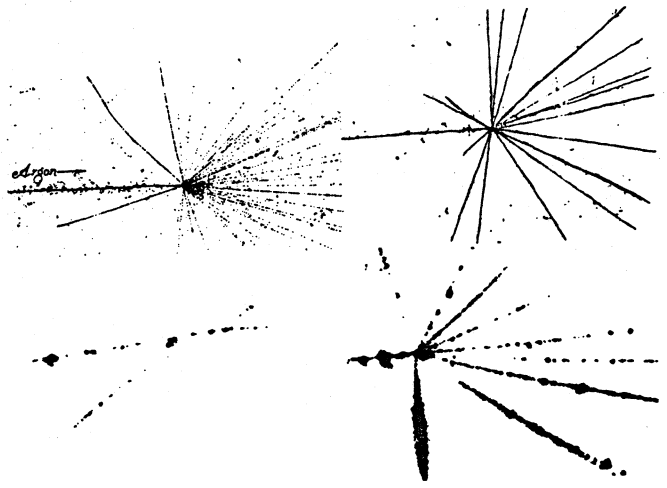

FIG. 2. Streamer chamber (lower) and emulsion (upper) photographs of events in heavy-ion collisions. Bottom frames show examples of few and many particle final states for ^{12}C + ^{20}Ne at 25 MeV/u. The top frames illustrate explosive events with ^{40}Ar at 1.8 GeV/u (left) and ^{12}C at 91 MeV/u (right).

The importance of intermediate energy collisions also becomes clear from the overview[4]) of reaction processes shown in Fig. 3. The reaction cross section as a function of energy is subdivided in the characteristic mechanisms for a typical system like ^{40}Ar on ^{232}Th. The vertical scale can also be regarded as a rough measure of impact parameter. At low energies, central collisions lead to complete

fusion, whereas peripheral collisions produce deep-inelastic scattering. The division appears to be set by a critical radius[5] where the nuclei overlap at their half density points, i.e. $R_c \simeq 1.0\,(A_1^{1/3} + A_2^{1/3})$fm, but the division is not sharp in all cases[6]. The magnitude of the reaction cross section is given by $\pi R^2(1-V/E)$, with $R = r_o(A_1^{1/3} + A_2^{1/3})$ and V is the Coulomb Barrier. At high energies there is growing evidence that the cross section falls below the geometrical limit πR^2, by about 20%, a phenomenon attributed to nuclear transparency.[7] The variation of the cross section appears to be well accounted for by a Glauber model calculation which superimposes the individual nucleon-nucleon collisions. It is important to note, however, that processes occur at high energies for which it would be unproductive to attempt an understanding in terms of nucleon-nucleon collisions. Thus deep-inelastic reactions are replaced by faster processes creating participants and spectators, whereas it is likely that central collisions lead to explosive events. The nuclei no longer stick together but are torn apart with varying degrees of violence as indicated on the figure. Nevertheless the division between peripheral and central reactions may continue to be defined by the critical overlap of nuclear matter.[8]

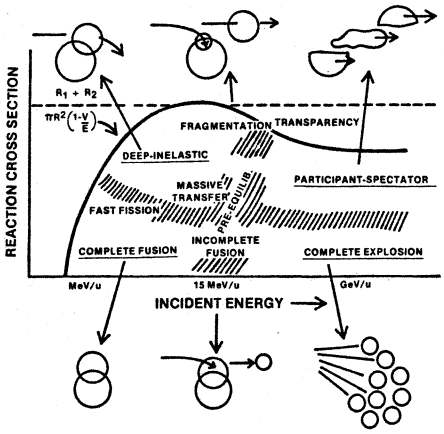

FIG. 3. Schematic illustration of heavy-ion collision processes, as a function of impact parameter (vertical scale) and energy/nucleon (horizontal).

There are intimations of these high energy phenomena already at 15 MeV/u, which is therefore a convenient starting point for the study of intermediate energy collisions.[8] The production of spectators is preceded by a rapid onset of fragmentation,[9] in which a large part of the projectile escapes, and the residual piece is captured or interacts strongly with the target, as established in many coincidence experiments.[10] For central collisions the complementary behaviour is observed: a substantial portion is captured[11,12] or undergoes deep-inelastic scattering[13] and a light particle is promptly emitted. As a function of impact parameter, a conceptual link can be established through an increasingly massive transfer up to incomplete fusion,[14] and indeed recent measurements have shown that the angular momentum (or impact parameter) is fractionated according to the mass transfer.[15] In these reactions parts of the colliding nuclei escape immediately, marking the onset of preequilibrium phenomena and of processes similar to higher energy reactions in which a larger number of particles is produced. The boundary between the low and high energy sections of the diagram appears to be around 15-20 MeV/u.

One explanation[16,17] comes by using the balance of nuclear, Coulomb and centrifugal forces to determine the critical angular momentum l_c:

$$4\pi\gamma\frac{R_1R_2}{R_1+R_2} = \frac{Z_1Z_2e^2}{(R_1+R_2)^2} + \frac{l_c(l_c+1)\hbar^2}{\mu(R_1+R_2)^3} \quad .$$

One finds that at 15 MeV/u, the critical angular momentum for all fragments of the projectile (excepting possibly single nucleons) is exceeded; it is natural therefore to expect preequilibrium and fragmentation phenomena. The energy of 15 MeV/u is also close to the velocity of sound, determined from,

$$\frac{v}{c} = \sqrt{\frac{K}{9m}} \quad ,$$

with the compressibility constant K≈200-300 MeV, whereas 20 MeV/u is close to the mean Fermi energy of nucleons in a nucleus, viz.

$$\frac{3}{5}\frac{p_f^2}{2m} \quad .$$

Since the associated times are related to the relaxation of collective and single particle modes, it is therefore natural to expect a change in the nature of reactions when the collision time is shorter.

Ultimately, of course, one must seek an understanding of the boundaries in Fig. 3 in detailed theories of nuclear collisions. In Fig. 4 we compare two theoretical approaches of TDHF and hydrodynamics.[18-21]) On the left the outcome of a TDHF calculation for $^{12}C + ^{197}Au$ at 30 MeV/u is shown for central and periheral impact parameters of 1 and 6 fm. The outermost contour line has density $\rho = 0.14 \times 2^{-NC+1}$ nucleons/fm, and successive inner contours have densities increasing by a factor of 2. In the central collision, a high velocity jet of dilute matter (free nucleons) emerges, whereas for the peripheral collision, a large part of the projectile is captured and a few nucleons escape. There are similarities to massive transfer[11]) and to the emission of PEPS.[22])

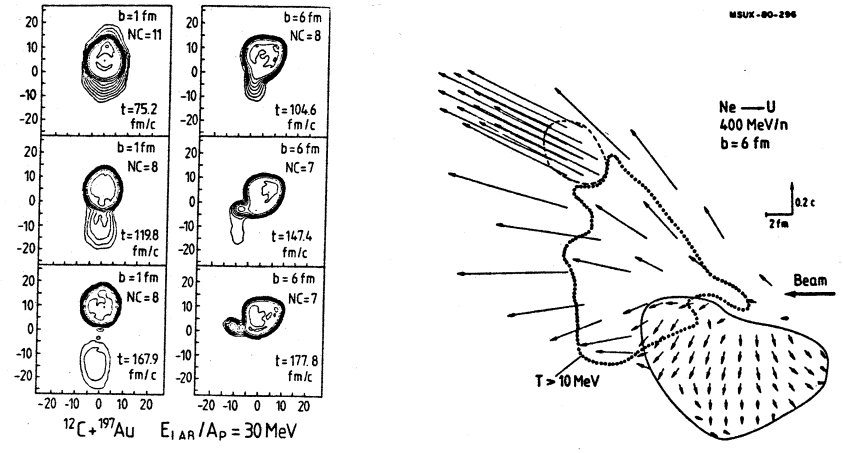

FIG. 4. Comparison of TDHF and hydrodynamical calculations of heavy-ion collisions. On the left are density contours for $^{12}C + ^{197}Au$ at 30 MeV/u (TDHF); on the right are temperature, density and velocity profiles for ^{20}Ne + U at 400 MeV/u (hydrodynamics).

On the right is shown the density, temperature and velocity profiles for a peripheral, hydrodynamical collision at a much higher energy of 400 MeV/u. A high velocity, low density (fragmented) projectile remnant can be identified, together with a low velocity target spectator and an intermediate velocity zone of high temperature reminiscent of the participants.[23]) Although the two theories start out from very different assumptions, in particular with very long and very short mean free paths,[21]) both theories contain elements of the truth determined from experiment. It is likely that phenomena at intermediate energies, which we now take to cover the region from 15-200 MeV/u, will constitute the best meeting ground for the various theoretical approaches. One challenge is to explain the boundaries between the various reactions in Fig. 3. We shall devote the remainder of this paper to a demonstration that there is experimental evidence for transitional phenomena. Intermediate energy experiments which relate to the onset of participant-spectator and of explosive mechanisms will be described.

3. Evolution of peripheral collisions

In order to study the transition to fragmentation and spectator reaction mechanisms, we look at the characteristic features of nuclei produced by the rapid shearing or abrasion process shown at the right of Fig. 4. Suppose[24]) that A nucleons of the projectile are assembled with zero net three momentum, $P_A = 0$. If F of these nucleons, chosen at random, are suddenly released as a single fragment, what would be the mean square total momentum P_F? The A nucleons have mean square momentum $\langle p^2 \rangle$, correlated by the requirement $P_A = 0$, so that,

$$A\langle p^2 \rangle + \sum_{i \neq j} \langle pi \cdot pj \rangle = 0$$

or

$$\langle\langle pi \cdot pj \rangle\rangle = -\langle p^2 \rangle / A-1.$$

where the double bracket denotes an average over all $i \neq j$. Then we get,

$$P_F^2 = \langle\langle \left(\sum_{i=1}^{F} p_i \right)^2 \rangle\rangle = \frac{F(A-F)}{(A-1)} \langle p^2 \rangle$$

and $\langle p^2 \rangle$ is just the mean square momentum associated with the Fermi motion of the nucleons, i.e. $3/5\ p_f^2$. Therefore a measurement of each Cartesian component of the momentum distribution of fragments released by the abrasion process will yield a gaussian distribution of the form $\exp(-p^2/2\sigma^2)$, where

$$\sigma^2 = \frac{p_f^2}{5} \frac{F(A-F)}{A-1} = \sigma_o^2 \frac{F(A-F)}{A-1} \quad .$$

Striking verification comes from experiments with Argon at 213 MeV/nucleon.[25]) The spectrum for a typical fragment ^{34}S is shown in Fig. 5, which has indeed a distribution of gaussian form, peaked at an energy corresponding closely to the fragment travelling with the velocity of the incident beam, as we expect for a spectator projectile fragment. In fact the velocity at the peak is slightly less (6850 MeV instead of 7242 MeV); some reduction is expected on account of the separation energy.[8]) The values of σ_o deduced from a gaussian fit to the peak in momentum space, as well as to all the other observed fragments between Z=8 and 16, are shown at the bottom of the figure. The values are remarkably constant with a mean of σ_o = 94 MeV/c, which correspond to p_f = 210 MeV/c, instead of a Fermi momentum[26]) of 250 MeV/c, determined in electron scattering. The difference may be due to the fact that electrons and heavy ions probe different regions of the nucleus.[27])

This type of experiment has been carried out for several projectiles, covering a wide range of energies up to 2 GeV/u. The values of σ_o are plotted in Fig. 6 as a

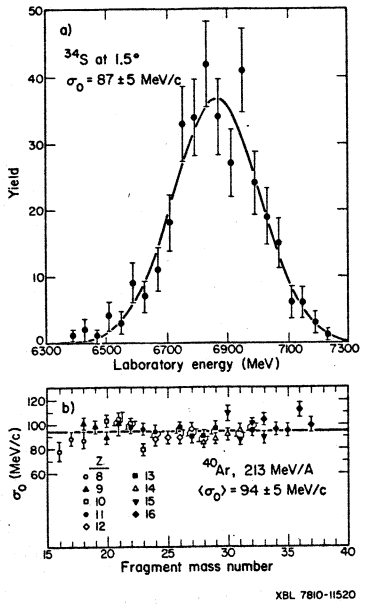

FIG. 5. The upper section shows the energy spectrum for ^{34}S fragments produced by ^{40}Ar on ^{12}C at 213 MeV/u. The widths of the momentum distributions σ_o (see text) for all observed fragments are shown below.

function of incident energy by the line labelled "spectators" using the momentum scale on the right. Most of the results come from ^{16}O on Au and Pb [8,9] in addition to the point for ^{40}Ar + ^{12}C discussed above and for ^{12}C + Au [28] at 86 MeV/u. Experiments with alpha particles above 20 MeV/u also confirm the importance of fragmentation. [29-31] It is plausible to identify the spectator fragments down to 15 MeV/u by the signature of a constant momentum width, [32] which reflects the Fermi motion or, strictly speaking, the ground state motion of abraded fragments cut loose from the parent nucleus. More sophisticated analyses of these reactions have attempted to extract the influence of ground state correlations in the zero point motion. [25,33,34]

The sudden decrease of the momentum widths at energies below 15 MeV/u implies a change in the reaction mechanism. As indicated on Fig. 3, the unseen fragment is then more likely to be transferred to the target, imposing through momentum conservation a constraint on the momentum distribution of the observed fragment. [35] A detailed understanding of the transition in Fig. 6 must ultimately come from a microscopically based theory. Indeed there has been some progress towards this goal by means of direct reaction theories of projectile fragmentation, [31,35] two-body transfer reactions, [36,37] surprisal analysis, [38] and incomplete fusion. [11,16,17] All of these approaches [39] infer a transitional behaviour in the region of 15 MeV/nucleon. It has also been shown [40] using perturbation theory that the transition probability for a heavy-ion reaction leads to an expansion for the cross section in terms of y, the ratio between the duration of a nucleon-nucleon collision and the elasped time between two successive interactions. There is a Markovian part independent of y and a non-Markovian part containing an explicit y-dependence. This decomposition shows that a transition from Markovian behaviour occurs around 20 MeV/nucleon.

Although we have discussed only one Cartesian component of the momentum distribution in the direction parallel to the incident beam, the theory predicts equal dispersions in the perpendicular components, in agreement with experimental

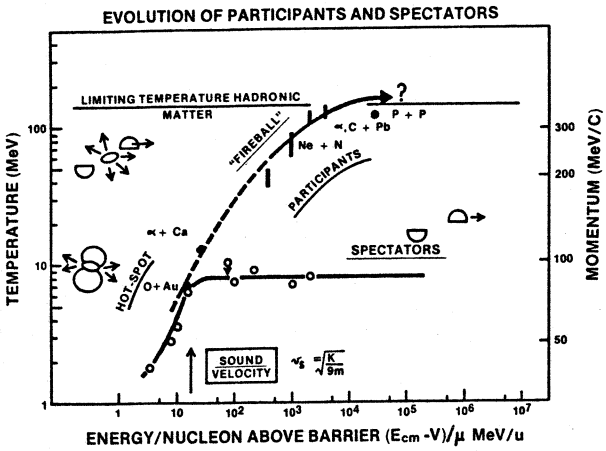

FIG. 6. Plot of the momentum widths of spectator fragment distributions (right hand scale) as a function of the energy/nucleon above the barrier. The temperature of the nuclear fireball and of hot spots are shown by the scale at the left.

data at 2.1 GeV/u. At energies in the vicinity of 100 MeV/u however, the perpendicular momentum distribution becomes much wider.[28,41]) Current explanations proceed along the lines of deflection of the fragments by the Coulomb, nuclear -and possibly compressional - potentials[41]) as well as of recoil effects due to the rescattering of participant nucleons into the spectators.[28]) Measurements of target recoil momenta indicate that several nucleons are captured in experiments with ^{12}C at 86 MeV/u.[18]) These effects should eventually be accounted for quantitatively by the TDHF and hydrodynamic models discussed for Fig. 4, and may constitute a useful method for testing the applicability of such models.[18])

4. Evolution of central collisions

We turn now to a consideration of the participants,[42]) which represent the overlapping regions of the collision. In relativistic nuclear reactions, this region can be highlighted by imposing the additional constraint that a high multiplicity of charged particles be registered in an array of tag counters.[43]) with this trigger the coincident light particles have energy spectra of exponential form, $\exp(-E/T)$ from which the temperature of the participant zone, the nuclear fireball[47]), can be deduced. Temperatures for the emission of nucleons and pions have been measured[48]) for a wide variety of colliding systems from energies of 200 MeV/u up to 3.6 GeV/u. In order to display the results on Fig. 6, we note that the Gaussian momenta distribution for the spectators, $\exp(-p^2/2\sigma^2)$, can be transformed to an energy distribution with $T \approx \sigma_o^2/m$ and the limiting momentum width is then equivalent to a limiting energy width of approximately 8 MeV (see scale on left hand side).

The temperatures for the participant zone, or fireball, are shown in Fig. 6 by the vertical bars. These do not represent errors, but rather the range of temperatures deduced for different initial systems and different final state particles; one characteristic system is indicated. These differences are intriguing per se, and may be evidence for collective and hydrodynamical effects,[46]) but our present interest is more in the overall smooth trend, which reaches a temperature close to 140 MeV, the "boiling point of hadronic matter". This limiting temperature exists in the case of an exponential growth of particles which, by their creation, prevent further increase of random kinetic energy in the fireball.[47]) The clear existence of this limit must await future experiments on higher energy accelerators, although we note that a similar temperature is deduced for the hadronic fireball in p+p collisions at much higher energies.[48])

The theoretical description of the temperature evolution will answer important questions on the extent of thermalisation, on whether the participants constitute an ideal or a Fermi gas,[49] and on the contributions of collective hydrodynamical[46] effects on the one hand or of single nucleon knock out on the other.[50-52] It becomes of interest then to explore the validity and the limits of this participant model at lower energies.

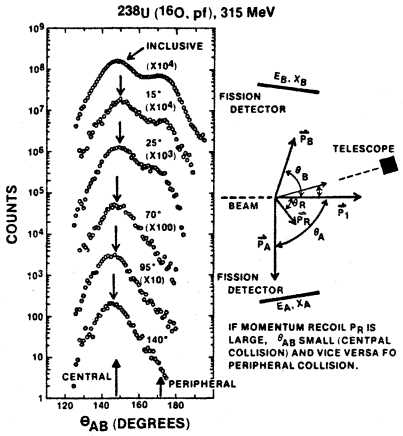

FIG. 7. Distribution of opening angle θ_{AB} of fission fragments produced by the reaction ^{16}O + U at 315 MeV for inclusive reactions (top) and in coincidence with forward protons at several angles.

As the incident energy is reduced the fireball becomes less well separated in velocity or rapidity from the spectators, and could eventually be trapped for the duration of the collision between the surrounding nuclei. In this spirit the logical extrapolation of the fireball is the hot-spot, for which there is growing experimental and theoretical justification.[53,54] Just as in relativistic collisions there is an advantage in selecting central events by means of multiplicity triggers, it is preferable also to make exclusive measurements at lower energies. A useful trigger is given[55,56] by the set-up of Fig. 7. Particles are detected in a ΔE-E telescope in coincidence with fission fragments from the residual heavy target. By measuring the angle θ_{AB} between the outgoing fission fragments as well as their energies, the recoil momentum can be deduced and the momentum balance reconstructed. In Fig. 7, the fission coincidence spectra are shown[57] as a function of θ_{AB} in an inclusive measurement (i.e. any particle detected in the forward telescope) and also for coincident protons detected over a wide range of angles (15° to 140°).

The existence of two peaks in the inclusive fission fragment distribution point to two dominant momentum transfers. The peak close to θ_{AB} = 173° (corresponding to the smaller transfer) is the only one appearing in coincidence with projectile-like fragments (Li-O); it is therefore associated with a peripheral process, which is known to be the main source of these particles.[8] The larger momentum transfer (θ_{AB} = 148°) is then attributed to a central collision. It follows that there is a sizeable probability for emission of fast protons in both peripheral and central collisions, but at backward angles only the central component persists. The arrows in the figure indicate the position at which the recoil momentum is equal to the difference between the mean momentum carried by the coincident light particle and the beam momentum. The agreement with the peak location suggests that the emission of only one energetic light particle is the most probable mechanism. This reaction is therefore an illustration of the incomplete fusion process discussed earlier.

The proton spectra associated with the central collision peak are shown in Fig. 8.[57] It is quite clear that they cannot originate from a classical compound nucleus. By extending up to energies of 80 MeV with substantial cross-section, they

require temperatures much too high: the center of mass energy of 200 MeV above the barrier leads to T = 2.9 MeV for the compound system, using $E^* \simeq \frac{A}{8} T^2$, and we expect a decrease of 10^9 in cross section between 10 and 70 MeV, compared to the observed factor of only 10^3. What type of source, one therefore asks, is responsible for this emission? Interpretations abound in the literature - and in the contributed papers to this conference-ranging from Fermi jets, PEPS[22]) (prompt emission of particles), deexicitation of the projectile,[58,59]) which can acquire high excitations by fluctuations[60]) in the deep-inelastic energy loss, and from pre-equilibrium emission.[61,62]) We shall describe only a simple two-parameter fit to the data, which emphasises the connection to the high energy phenomena and to hot-spots.[61,63]) This parameterization is in terms of a Maxwellian distribution at temperature T in a rest frame that moves with velocity v, parallel to the beam axis. Correcting for the Coulomb repulsion from the target, one obtains[57])

$$\frac{d^2N}{d\Omega dE} = N_o (E-E_c)^{\frac{1}{2}} \exp - \left[\frac{(E-E_c)+E_1-2E_1^{\frac{1}{2}}(E-E_c)^{\frac{1}{2}}\cos\theta}{T} \right]$$

where E_c is the kinetic energy gained Coulomb repulsion, $E_1 = \frac{1}{2}mv^2$ is the kinetic energy of a particle at rest in the moving frame and N_o is an overall normalization constant. The solid curves in Fig. 8 were calculated with E_c = 10 MeV, v = 0.09 c and T = 7 MeV. The velocity is close to the value 0.089c of the nucleon-nucleon center of mass frame if the slowing down of the ^{16}O nuclei in the field of the ^{238}U nucleus is taken into account. With equal participation from target and projectile nucleons, one obtains a temperature,

$$T = \frac{2mv^2 \varepsilon_F^{\frac{1}{2}}}{\pi^2}$$

where ε_F is the Fermi energy of 38 MeV and m the nucleon mass, giving T = 7.5 MeV. The data appear therefore to be consistent with emission from a hot-spot in which the thermalisation of the nucleon velocities occurs first in the nucleon-nucleon center of mass frame, and in which the time scale for particle emission is comparable to the time scale for energy and momentum transfer from the hot-spot to the target nucleus.

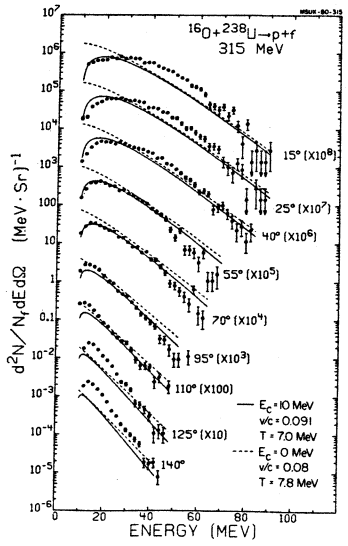

FIG. 8. Energy spectra of protons in coincidence with fission fragments for reactions of ^{16}O + U at 315 MeV. The solid line is a theoretical fit discussed in the text. The dashed line illustrates the effect of varying parameters.

The relationship of this description to the high energy fireball model[44]) as well as to the low energy microscopic pre-equilibrium theories[61,62]) is clearly of interest. For the present we merely emphasise the possible continuity in the description by adding this localised source temperature to the scheme of Fig. 6, together with a point deduced in a similar analysis of α induced reactions.[64]) The diagram suggests that localised regions of excitation may be observable in the vicinity of 20 MeV/u. (There are also several experiments on light particle emission at lower incident energies which show evidence for hot-spot formation.[53,65-67]) As shown in Fig. 6 this transition would then coincide with the onset for the production of spectator fragments, and occurs at an energy corresponding closely to the velocity of sound. It may be that the conditions for forming localised regions of excitation are met when this velocity is exceeded, since the relaxation time for spreading the initial energy deposition must be linked to the sound and Fermi velocities.

Theoretical models of hot-spot formation have been derived not only for the data of Fig. 8,[68-70]) but for a variety of heavy-ion induced reactions at lower energies,[71,72]) as well as for light-particle induced reactions.[73,74]) These approaches show that, above the sound velocity, the hot-zone could be formed at greater than normal nuclear density,[75]) thereby perturbing the trend of the energy-temperature relationship. Basic to the theory is the existence of a short mean free path,[76-78]) a requirement also essential to hydrodynamic models. A clear demonstration of hot-spot formation is therefore of some importance for the theory of nuclear collisions, since it demonstrates a transition from the long mean free path of the TDHF approximation, to the short mean free path and the two-body collisions required by hydrodynamics.[79-82]) A recent calculation of the mean free path is shown[78]) in Fig. 9 for a nucleon in a Fermi gas as a function of the energy above the Fermi energy, and for different temperatures. The T=0 curve is in approximate agreement with the trend of values deduced[73,74]) from the optical model imaginary potential W,

$$\lambda = \frac{1}{W}\sqrt{\frac{(\hbar c)^2 E}{2mc^2}} \quad .$$

Here the incident energy is augumented by the real potential depth, taken as 40 MeV. We see that the values of λ are long compared to nuclear dimensions at low temperatures, but they rapidly decrease with increasing temperature, approaching the classical high energy limit of $1/\rho\sigma \approx 2$fm at T = 10 MeV. This reduction is due to the diminished significance of the Pauli blocking, which could offer an explanation for hot-spot formation at energies in the vicinity of 20 MeV/u, where the temperature of the source is close to 8 MeV.[83]) It has also been shown that at incident energies close to 80 MeV/u, the longitudinal momentum decay length is only 1.5 fm.[84]) Thus in this energy region if a hot-spot is created, it should be stopped quickly, and the zone might emit nucleons before the equilibration with the surrounding nuclear medium is achieved. A hot-spot model has been used successfully to discribe intermediate energy proton collisions,[73]) and even for studies of hadronic matter in high energy proton-proton collisions at 100 GeV/c.[85]) Here hydrodynamic concepts are invoked such as the conductivity and transport properties of hadronic matter in the same way that we might now apply them to nuclear matter.[71,72]) Additional information about hot-spots can be obtained from the emission of other complex light particles, and these we discuss in the next section.

5. Emission of light composite particles

There are two current approaches to the problem of light composite particle emission in relativistic heavy-ion collisions.[86]) Since these approaches can also give information on the dimensions of a localized zone, we describe their physical content before applying them to the intermediate energy data.

The coalescence model[87,88]) determines the probability for condensation of nucleons, which takes place if they are within a coalescence radius p_o of each other. The probability of finding a nucleon in a sphere of momentum radius p_o, centered at p is:

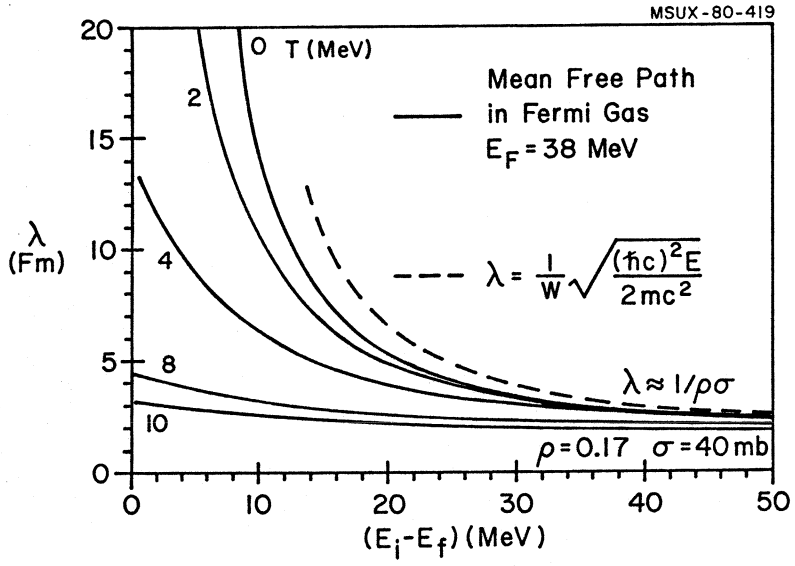

FIG. 9. Theoretical predictions of the mean free path of a nucleon as a function of energy above the Fermi energy are shown for several nuclear temperatures. The trend of experimental data on mean free paths deduced from the imaginary part of the optical potential is given by the dashed line.

$$P \simeq \left(\frac{4}{3}\pi p_o^3\right) \frac{d^2\sigma_1(p)}{p^2 dp d\Omega}$$

where $d^2\sigma_1/p^2 dp d\Omega$ is the cross section for emission of a single nucleon. Then the probability for finding A nucleons is just:

$$P_A \simeq \left(\frac{4}{3}\pi p_o^3\right)^A \left(\frac{d^2\sigma_1}{p^2 dp d\Omega}\right)^A$$

To obtain the cross section, we take the probability of finding (A-1) nucleons in the sphere p_o and multiply by 1/A times the cross section for emission of the additional particle. The final expression, with the correct constant factors is:

$$\frac{d^2\sigma_A}{p^2 dp d\Omega} = \frac{1}{A!}\left(\frac{4\pi p_o^3}{3\sigma_o}\gamma\right)^{A-1}\left(\frac{d^2\sigma_1}{p^2 dp d\Omega}\right)^A$$

where σ_o is the total reaction cross section, and γ is the relativistic correction factor. Once the cross section σ_1 for single nucleon emission is known, the cross section for any other composite fragment (d,t, ^{3}He, etc.) is readily calculated, with the addition of one parameter, the coalescece radius.

Paradoxially this power law dependence on the single nucleon cross section is also expected in a thermodynamic model.[88] Then the cross section for emission of a fragment is given by exp(-E/T) which can be written as,

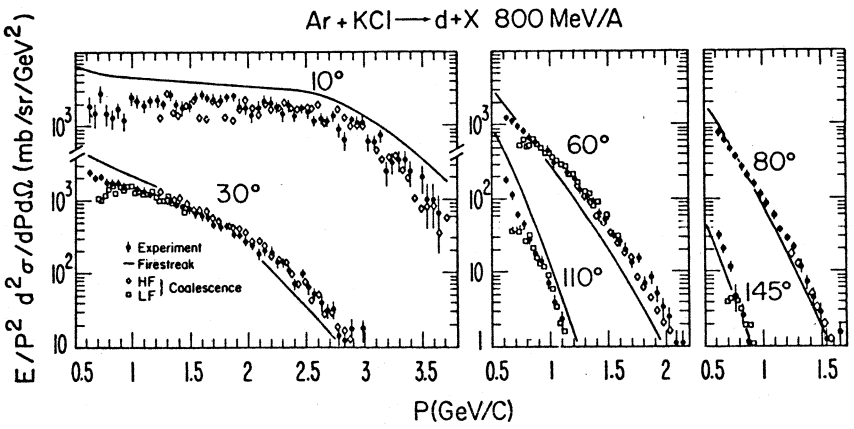

FIG. 10. Comparison of momentum spectra for deuterons produced in the reaction of Ar on KCl at 800 MeV/u with the coalescence model. The solid line is the prediction of a thermal firestreak model (see Ref. 89).

$$\exp\left(\frac{-E/A}{T}\right)^{A},$$

i.e. the single nucleon cross section raised to the power A, at the same energy per nucleon. In spite of this equivalence the physics content of the two models is quite different. The coalescence radius is an intrinsic property of the emitted particle and consequently should be independent of the energy or mass of the colliding system. The equivalent constant in the thermodynamic model is related to the largest volume in which thermodynamic and chemical equilibrium is maintained. As such, it is a property of the emitting region and may depend on the size of the nuclei forming it. Apart from some constants and statistical weighting factors the parameters of the two models are related by,

$$V \propto h^3/p_o^3.$$

The power law dependence is obeyed with remarkable accuracy at relativistic energies. Fig. 10 gives[89]) an example for the reaction $^{40}Ar + {}^{208}Pb \rightarrow d$ at 800 MeV/nucleon, with a coalescence radius of 213 MeV/c. Expressing the volume in the thermodynamic model in terms of the radius of an equivalent sphere,

$$R = a(A_1^{1/3}+A_2^{1/3})+b$$

with a = 0.24 and b = 1.9 fm for deuterons and 1.5 fm for tritons and ^{3}He, values of R in the range of 3.5 - 4 fm are deduced. The application of these prescriptions to lower energy data, for the ^{16}O induced reactions at 15 MeV/u[57]) and for α particle reactions at 25 and 43 MeV/u,[64,90]) also gives surprisingly good fits as shown in Fig. 11. In the case of α particle reactions, the production of ^{6}Li is described by raising the nucleon cross section to the sixth power.

The important physics comes from the trends of the coalescence radius, or alternatively of the radius of the emitting volume, as a function of energy. These are shown in Fig. 12, in which the vertical bars represent the range of values deduced for different emitted final particles (d,t,^{3}He). The data above 200 MeV/u are from ^{12}C or ^{20}Ne induced reactions,[89]) the lowest energy point at 15 MeV/u is from $^{16}O + {}^{238}U$,[57]) and the remaining two are from alpha induced reactions.[90]) In

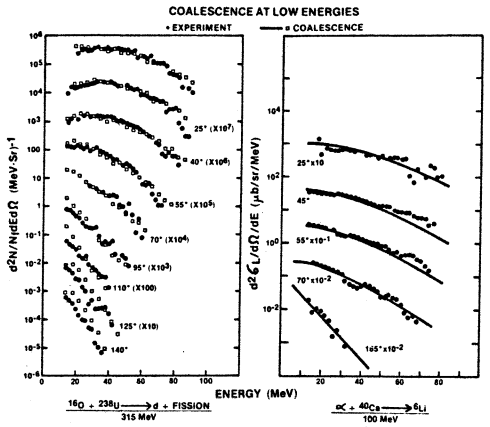

FIG. 11. Comparison of experimental data for $^{16}O + U \rightarrow d$ at 315 MeV (left) and $\alpha + Ca \rightarrow {}^{6}Li$ at 100 MeV (right) with the coalescence model.

order to compare results for different particles the coalescence radii plotted in Fig. 12 are adjusted to take into account the statistical spin weighting factors.[89] Once again we find a uniformity of description from 2.1 GeV/u down to the region of 15 MeV/u, after which the coalescence radius rapidly decreases, or alternatively the radius of the emitting zone increases. There are indications that the coalescence radius depends systematically on the size of the colliding system[91] possibly favoring the thermodynamic interpretation. Additional evidence comes from the agreement between the radii deduced from complex fragment emission with the values derived from two-pion[92,93] and two-proton interferometery,[94] as indicated in Fig. 12. At the low energy end the volume of the hot-zone also turns out[68-70] to be of the order of 4 fm. Whatever the ultimate interpretation of these phenomena, it seems likely that the required uniformity of description over several decades in energy will impose useful constraints on any theory. We should note that in light ion induced reactions, the coalescence model has also been applied. There the systematic dependence of the coalescence radius on the emitted particle does not favor the thermodynamic interpretation.[95]

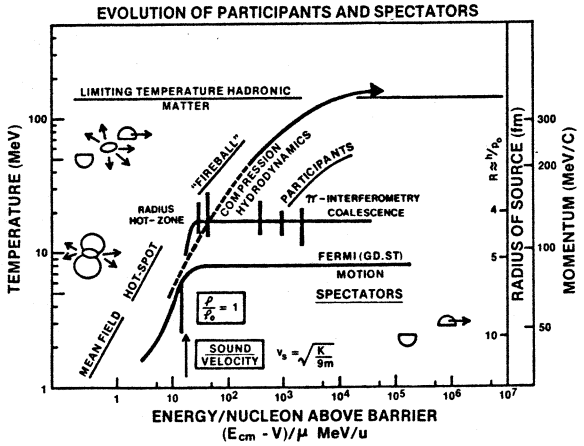

FIG. 12. The variation of coalescence radii, or alternatively of thermal source radii (right hand scales) with energy is added to the trends of Fig. 6. Possible characteristic phenomena in different domains are labelled.

An additional unknown at the present time is the extent of equilibration that takes place in the participant region, over the full range of energy displayed in Fig. 12. At high energies there are experiments which show that a substantial fraction of the emitted nucleons is produced by a single nucleon-nucleon collision.[50,96] This conclusion is supported by detailed cascade calculations.[52] There are also indications that low energy pre-equilibrium emission may be dominated by single scattering for[97] nucleon induced reactions. It is obviously important to study this problem over a broad energy region to ascertain whether the labels assigned to Fig. 12 are completely justified! To deal with these questions requires more detailed experiments on two or few-body correlations, which can in principle distinguish the effects of hydrodynamics and single scattering.[98] The apparatus required is likely to be of a complexity comparable to that described in the next section.

6. Peripheral and central collisions

So far we have discussed the onset of the spectator and participant processes illustrated in Fig. 3, which appears to occur at fairly low energies. In this final section we discuss an experiment suggesting that explosive central collisions may also set in at relatively low energy. The apparatus used[99] is illustrated in Fig. 13. Forward going light fragments could be registered in any array of scintillators. Heavy fragments were detected in the position sensitive hodoscope of avalanche counters covering a solid angle of 2.5 sr. Recoil target fragments could be identified with the multiple ion chamber, combined with time-of-flight avalanche counters.

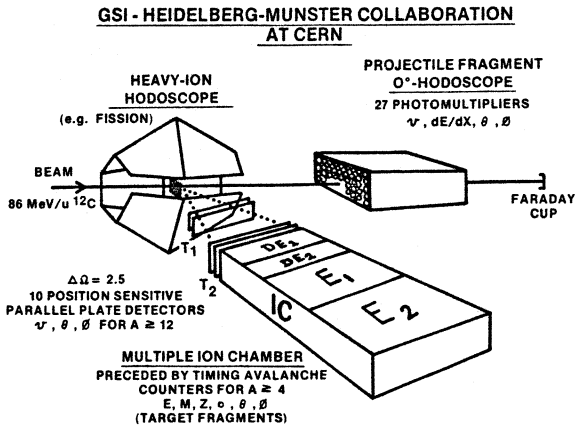

FIG. 13. Experimental apparatus for the study of reactions induced by ^{12}C at 86 MeV/u.

We shall describe one aspect of an experiment with this apparatus, the detection of fission fragments in coincidence with forward going light particles, produced by 86 MeV/u ^{12}C beams or a Uranium target. The distribution of opening angles of the fission fragments associated with 0, 1 or 2 light particles is shown at the top of Fig. 14. The results can be compared directly with the experiment[57] of ^{16}O on Uranium at the lower energy of 20 MeV/u which we discussed earlier (see

Fig. 7). Whereas in the latter case fission fragments were generated in both central and peripheral collisions, at the higher energy only the peripheral group remains. The inference is that central collisions at 86 MeV/u have led to a more violent disruption of the nuclei. Similar conclusions have been drawn from experiments at still higher energies of 400 MeV/u.[10] It remains to map out the disappearance of the fission component in full momentum transfer collisions, and to establish if the boundary exists in the region of 15-25 MeV/u indicated on the overview of reaction mechanisms in Fig. 3. Of equal interest is the division between the participant-spectator peripheral reactions and the central explosive reactions as a function of impact parameter. There are indications that the peripheral processes span a region of impact parameters down to a radius similar to the critical value dividing low energy fusion and deep-inelastic scattering.[6,8]

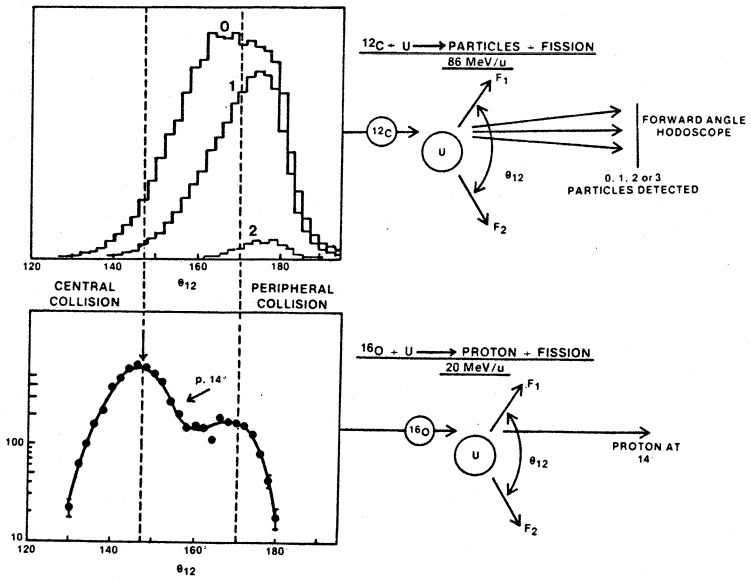

FIG. 14. Comparison of the distribution of the opening angles of fission fragments in coincidence with forward going light particles for ^{12}C + U at 86 MeV/u (top) and ^{16}O + U at 315 MeV (bottom).

The origin of explosive events is of considerable importance in heavy-ion collisions. We recall that they certainly occur at energies between 25 and 90 MeV/u (see Fig. 2). It may be that these events are related to the instability of the hot-zone which we have discussed in this paper.[101] When the excitation energy per nucleon in an interacting volume of nucleons composed of a_1 nucleons from the projectile and a_2 from the target, viz,

$$E^* = E_{LAB} \frac{a_1 a_2}{(a_1+a_2)^2},$$

exceeds 8 MeV the system ($a_1 + a_2$) will disintegrate. If equal numbers of nucleons from the target and projectile participate $a_1 = a_2$ and E^*_{LAB} = 32 MeV/u. A more refined calculation with a proper treatment of surface and volume effects, places the explosion between 30 and 50 MeV/u, corresponding to hot-spot temperatures of 18 to

23 MeV, ignoring any effects of compression[75]). This energy region lies in the gap where there are no detailed available data. (See Figs. 6 and 12). In nuclear emulsions the probability of explosive events has been studied, from which it is found that there is a rapid increase up to 200 MeV/u followed by an apparent levelling off up to energies of 2.1 GeV/u.[102,103]) This type of study could be useful in determining the densities and temperatures of exploding nuclear matter as a function of energy. Perhaps it will be possible to compare the results with theoretical equations of state.[75,104]) The disintegration can also be studied in the TDHF method, in which the overlapping region of the two nuclei produces a rapid increase in density and an associated increase in the mean field potential.[79,82]) The appearance of this potential - the volcano effect-causes some of the nucleons to become unbound. This effect in turn lowers the depth of the self consistent potential, leading to a disintegration of one of the nuclei. The type of phenomena we have discussed in this paper may therefore offer an alternative to the high energy side-splash effects[105]) for the study of hydrodynamics and compressions. There may even be some advantage in experiments in the 20-200-MeV/u region, since high compressions can be achieved in the presence of much lower temperatures than at relativisitic energies.

7. Conclusion

In this brief survey of the initial experiments, I hope I have been able to convey the spirit and scope of research in intermediate energy nuclear collisions. The existing map - like the medieval maps of the world - is crude, with only the outlines of the major continents staked out. Likewise the theoretical descriptions are crude, reminiscent of a phlogiston theory in comparison to the precise theories of low energy nuclear physics. Nevertheless some of the paths we must follow in future research are already visible.

So far the field of intermediate energy has enjoyed a symbiotic relationship with its low and high energy hosts, drawing liberally from both. But the stability of theoretical descriptions over two or three decades in energy was unexpected, and will surely be valuable in refining the final descriptions. In the search for exotic phenomena such as phase transitions at high energies, the constraints imposed by demanding a successful description of the normal behaviour over a broad energy range may be very useful. For example, at high energies the entropy production in the nuclear fireball has been determined from the production ratio of deuterons and protons.[106]) An anomalously high value could be a signature of a phase transition. We have shown that the mechanism of deuteron and proton production may be very similar over an energy range from 15 MeV/u to 2100 MeV/u, and therefore it will be possible to check theories of the entropy production under "normal" conditions. Equally valuable will be the insights gained by grafting the precise, sophisticated approaches of low energy nuclear physics such as direct and multistep reaction theory, TDHF theory, microscopic pre-equilibrium theory onto the more macroscopic, phenomenological theories like hydrodynamics. It was one object of this paper to show that the marriage must take place in the vicinity of 15-20 MeV/u. But, of greater general significance, the intermediate energy region has sufficient richness to merit closer theoretical attention in its own right. It is neither quantal or classical, neither one-body or multibody, neither adiabatic or sudden, and it may finally demand the development of quite new theoretical methods.[106])

Acknowledgments

I wish to thank the many research workers who freely supplied their results and interpretations of experiments on intermediate energy nuclear collisions. Even though the limits of space and time did not permit the explicit inclusion of all this work, many of the ideas have nevertheless found their way into the manuscript. The preparation of this paper was supported by the National Science Foundation under Grant No. Phy 78-22696. Finally, it is a pleasure to thank Betty McClure for typing and assembling the manuscript.

References

1. K. Van Bibber, W. Pang, M. Avery and E. Bloemhof, LBL Preprint 9979; Proc. of Symposium on Heavy Ion Physics from 10 to 200 MeV/u, Brookhaven Report BNL-51115 (1979) p 365.
2. H. Heckman, Private communication. Other examples are given by L.S. Schroeder, Nucl. Inst. Meth. 162 (1979) 395.
3. J.P. Bondorf, Proceedings of the Conference on Large Amplitude Collective Nuclear Motion, Lake Balaton, (1979) p. 482.
4. J.P. Bondorf, Proc. of the Workshop on High Resolution Heavy Ion Physics, Saclay, (1978) p. 37.
5. D. Glas and U. Mosel, Nucl. Phys. A237 (1975) 429.
6. L. Adler, P. Gonthier, J.H.K. Ho, A. Khodai, M.N. Namboodiri, J.B. Natowitz and S. Simon, Phys. Rev. Lett. 45 (1980) 696.
7. N.J. DiGiacomo, R.M. Devries and J.C. Peng, Phys. Rev Lett. 45 (1980) 527 and refs. therein. See also contribution to this conference, p. 423.
8. C.K. Gelbke, C. Olmer, M. Buenerd, D.L. Hendrie, J. Mahoney, M.C. Mermaz and D.K. Scott, Phys. Reports 42 (1978) 312.
9. D.K. Scott, M. Bini, P. Doll, C.K. Gelbke, D.L. Hendrie, J.L. Laville, J. Mahoney, A. Menchaca-Rocha, M.C. Mermaz, C. Olmer, T.J.M. Symons, Y.P. Viyogi, K. Van Bibber, H.H. Wieman and P.J. Siemens, LBL Preprint 7729.
10. M. Bini, C.K. Gelbke, D.K. Scott, T.J.M. Symons, P. Doll, D.L. Hendrie, J.L. Laville, J. Mahoney, M.C. Mermaz, C. Olmer, K. Van Bibber and H.H. Wieman, Michigan State University Preprint, 1980 and refs. therein.
11. T.T. Sugihara, Proceedings of Nobel Symposium 50, Sweden, 1980, to be published in Physica Scripta, and refs. therein.
12. P. Gonthier, H. Ho, M.N. Namboodiri, L. Adler, J.B. Natowitz, S. Simon, K. Hagel, R. Terry and A. Khodai, Phys. Rev. Lett. 44 (1980) 1384.
13. R.K. Bhowmik, E.C. Pollacco, N.E. Sanderson, J.B.A. England and G.C. Morrison, Phys. Rev. Lett. 43 (1979) 619.
14. J.R. Wu and I.Y. Lee, Phys. Rev. Lett. 45 (1980) 8.
15. J.H. Barker, J.R. Beene, M.L. Halbert, D.C. Hensley, M. Jaaskelainen, D.G. Sarantites and R. Woodward, Phys. Rev. Lett. 45 (1980) 424.
16. K. Siwek-Wilczynska, E.H. du Marchie van Vorthuysen, J. Van Popta, R.H. Siemessen and J. Wilczynski, Phys. Rev. Lett. 42 (1979) 1599.
17. J. Wilczynski, K. Siwek-Wilczynska, J. Van Driel, S. Gonggrip, D.C.J.M. Hageman, R.V.F. Janssens, J. Lukasiak and R.H. Siemssen, Phys. Rev. Lett. 45 (1980) 606.
18. H. Stocker, R.Y. Cusson, J.A. Maruhn and W. Greiner, to be published.
19. H. Stocker, J.A. Maruhn and W. Greiner, Phys. Rev. Lett. 44 (1980) 725.
20. R.Y. Cusson, J. Maruhn and H. Stocker, Z. Phys. A294 (1980) 257.
21. H. Stocker, R.Y. Cusson, J.A. Maruhn and W. Greiner, Z. Phys. A294 (1980) 125.
22. J.P. Bondorf, J.N. De, G. Fai, A.O.T. Karvinen, B. Jakobsson and J. Randrup, Nucl. Phys. A333 (1980) 285.
23. S. Nagamiya, Nucl. Phys. A335 (1980) 517.
24. A.S. Goldhaber, Phys. Lett. 53B (1974) 306.
25. Y.P. Viyogi, T.J.M. Symons, P. Doll, D.E. Greiner, H.H. Heckman, D.L. Hendrie, P.J. Lindstrom, D.K. Scott, K. Van Bibber, G.D. Westfall, Phys. Rev. Lett. 42 (1979) 33.
26. E.J. Moniz, I. Sick, R.R. Whitney, J.R. Ficenec, R.D. Kephart and W.P. Trower, Phys. Rev. Lett. 26 (1971) 445.
27. J. Hufner and M.C. Nemes, Heidelberg Preprint, 1980.
28. C. Guet, M. Maurel, E. Monnand, J. Mougey, H. Nifenecker, P. Perrin, J. Pinston, C. Ristori, F. Schussler, M. Buenerd, A.J. Cole, D. Lebrun, J.M. Loiseaux, P. Martin, R. Ost, P. de Saintignon, H.A. Gustafsson, B. Jakobsson, T. Johansson, G. Johnsson, H. Krumlinde, I. Otterlund, H. Ryde, B. Schroeder, G. Tybell, J. Bondorf and O.B. Nielsen, Contribution to this conference, p 471.

29. J.R. Wu, C.C. Chang and H.D. Holmgren, Phys. Rev. Lett. 40 (1978) 1013.
30. J.R. Wu, H.D. Holmgren and R.W. Koontz, Phys. Rev. C20 (1979) 1284.
31. R. Shyam, G. Baur, F. Rosel and D. Trautmann, Phys. Rev. C19 (1979) 1246.
32. Similar trends have been reported by H. Homeyer, C. Egelhaaf, H. Fuchs, A. Gamp, H.G. Bohlen and H. Kluge, Proc. of Symp. on Heavy Ion Physics from 10 to 200 MeV/nucleon, Brookhaven National Laboratory Report BNL 51115 (1979) p. 769.
33. J.B. Bondorf, G. Fai and O.B. Nielsen, Phys. Rev. Lett. 41 (1978) 391.
34. D.J. Morissey, Proc. of Symposium on Heavy Ion Physics from 10 to 200 MeV/nucleon, Brookhaven National Laboratory Report BNL 51115 (1979) p. 821.
35. K.W. McVoy and C. Nemes, Z. Phys. A295 (1980) 177.
36. T. Udagawa, T. Tamura, T. Shimoda, H. Frolich, M. Ishihara and K. Nagatani, Phys. Rev. C20 (1979) 1949.
37. D.F. Jackson, Phys. Lett. 71B (1977) 57.
38. Y. Alhassid, R.D. Levine, S.G. Steadman, and J.S. Karp, Phys. Rev. C20 (1979) 1789.
39. For a summary, see C.K. Gelbke, Proceedings of the Symposium on Continuum Spectra in Heavy Ion Collisions (San Antonio, 1979).
40. F.S. Hernandez and G. Mantzouranis, Phys. Rev. C22 (1980) 575.
41. K. Van Bibber, D.L. Hendrie, D.K. Scott, H. Wieman, L.S. Schroeder, J.V. Geaga, J.A. Chessin, R. Treuhaft, J.Y. Grossiord, J.O. Rasmussen and C.Y. Wong, Phys. Rev. Lett. 43 (1979) 840; see also R. Legrain, T.C. Awes, H.J. Crawford, C.K. Gelbke, D.E. Greiner, H.H. Heckman, J.M. Kidd, P.J. Lindstrom, J. Mahoney, D.K. Scott, T.J.M. Symons and G.D. Westfall, Contribution to this Conference, p. 532.
42. S. Nagamiya and D.J. Morissey, LBL Preprint 10461, to be published in to Phys. Lett. B.
43. W.G. Meyer, H.H. Gutbrod, Ch. Lukner and A. Sandoval, Phys. Rev. C22 (1980) 179.
44. J. Gosset, J. Kapusta and G.D. Westfall, Phys. Rev. C18 (1978) 844 and refs. therein.
45. H. Stocker, A.A. Ogloblin, W. Greiner, G.S.I. - Preprint 79-19 (1979).
46. P.J. Siemens and J.O. Rasmussen, Phys. Rev. Lett. 42 (1979) 880.
47. K.K. Glendenning and Y.J. Karant, LBL Report 8653 and to be published in Nucl. Phys. A.
48. A.T. Laasanen, C. Ezell, L. Gutay, N.W. Schreiner, P. Schubelin, L. von Linder and F. Turkot, Phys. Rev. Lett. 38 (1977) 1.
49. H. Stocker, J. Hofmann, J.A. Maruhn and W. Greiner, Lectures at Erice School on Heavy Ion Interactions at High Energies, Prog. Part. and Nucl. Phys. Vol. 4, 1980.
50. S. Nagamyia, M.C. Lemaire, S. Schnetzer, H. Steiner and I. Tanihata, Phys. Rev. Lett. 45 (1980) 602 and refs. therein.
51. B.K. Jain, Phys. Rev. C22 (1980) 583.
52. M. Chemtob and B. Schurmann, Nucl. Phys. A336 (1980) 508 and refs. therein.
53. For a recent survey see D.K. Scott, Proc. of Int. School on Nuclear Structure, Alushta, Crimea, 1980 to be published.
54. For a discussion see W. Schroder, Proceedings of the Symposium on Continuum Spectra in Heavy Ion Collisions, San Antonio, 1979.
55. P. Dyer, T.C. Awes, C.K. Gelbke, B.B. Back, A. Mignerey, K.L. Wolf, H. Breuer, V.E. Viola Jr., and W.G. Meyer, Phys. Rev. Lett. 42 (1979) 560.
56. T.C. Awes, C.K. Gelbke, B.B. Back, A.C. Mignerey, K.L. Wolf, P. Dyer, H. Breuer and V.E. Viola Jr., Phys. Lett. 87B (1979) 43.
57. T.C. Awes, C.K. Gelbke, G. Poggi, B.B. Back, B. Glagola, H. Breuer, V.E. Viola and T.J.M. Symons, Phys. Rev. Lett. 45 (1980) 513.
58. See for example G.R. Young, R.L. Ferguson, A. Gavron, F.E. Obenshain, F. Plasil, M.P. Webb, C.F. Maguire and G.A. Petitt, Contribution to this Conference, p 602.
59. J.B. Ball, C.B. Fulmer, M.L. Mallory and R.L. Robinson, Phys. Rev. Lett. 40 (1978) 1698.

60. R.P. Schmitt, G.J. Wozniak, G.U. Ratazzi, G.J. Mathews, R. Regimbart and L.G. Moretto, Lawrence Berkeley Laboratory Preprint, 1980.
61. T.J.M. Symons, P. Doll, M. Bini, D.L. Hendrie, J. Mahoney, G. Mantzouranis, D.K. Scott, K. Van Bibber, Y.P. Viyogi, H.H. Wieman and C.K. Gelbke, Phys. Lett. 94B (1980) 131.
62. M. Blann, UCRL Preprint 84526, 1980.
63. D.K. Scott, Proceedings of the 1st Oaxtepec Conference, Instituto de Fisica, Vol. 1 (1978) p. 221.
64. H. Lohner, B. Ludewigt, D. Frekers, G. Gaul and R. Santo, Z. Phys. A292 (1979) 35.
65. L. Westerberg, D.G. Sarantites, D.G. Hensley, R.A. Dayras, M.L. Halbert, J.H. Barker, Phys. Rev. C18 (1978) 797.
66. H. Ho, R. Albrecht, W. Dunnweber, G. Graw, S.G. Steadman, J.P. Wurm, D. Disdier, V. Rauch and F. Schiebling, Z. Phys. A283 (1977) 235.
67. H. Utsunomiya, T. Nomura, T. Inamura, T. Sugitate and T. Motobayashi, Nucl. Phys. A334 (1980) 127 and refs therein.
68. S.I.A. Garpman, D. Sperber and M. Zielinska-Pfabe, Phys. Lett. 90B (1980) 53.
69. W.W. Morison, S.K. Samaddar, D. Sperber and M. Zielinska-Pfabe, Phys. Lett. 93B (1980) 279.
70. P. Mooney, W.W. Morison, S.K. Samaddar, D. Sperber and M. Zielinska-Pfabe, Preprint, 1980.
71. P.A. Gottschalk and M. Westrom, Nucl. Phys. A314 (1979) 232.
72. R. Weiner and M. Westrom, Nucl. Phys. A256 (1977) 282.
73. N. Stelte, M. Westrom and R.M. Weiner, Preprint 1980.
74. J.R. Wu, C.C. Chang and H.D. Holmgren, Phys. Rev. C19 (1979) 659 and 698.
75. S.I.A. Garpman, S.K. Samaddar, D. Sperber and M. Zielinska-Pfabe, Phys. Lett. 92B (1980) 56.
76. S.I.A. Garpman, D. Sperber and M. Zielinska-Pfabe, Phys. Lett B. to be published.
77. K.H. Muller, Phys. Lett 93B (1980) 247.
78. M.T. Collins and J.J. Griffin, Univ. of Maryland Preprint PP 80-072 (1980), to be published in Nucl. Phys. A.
79. C.Y. Wong, Symposium on Heavy Ion Physics from 10 to 200 MeV/nucleon, Brookhaven National Laboratory, BNL - 51115 (1979) p. 379.
80. A.R. Bodmer and C.N. Panos, Phys. Rev. C15 (1977) 1342; A.R. Bodmer, Proceedings of Conference on Theoretical Aspects of Heavy Ion Collisions, ORNL Report 770602.
81. P. Bonche, S. Koonin and J.W. Negele, Phys. Rev. C13 (1976) 1226.
82. H.H.K. Tang and C.Y. Wong, Phys. Rev. C21 (1980) 1846.
83. S. Kind and G. Patergnani, Nuovo Cimento 10 (1953) 1375.
84. M.I. Sobel, P.J. Siemens, J.P. Bondorf and H.A. Bethe, Nucl. Phys. A251 (1975) 502.
85. R.M. Weiner, Phys. Rev. D 13 (1976) 1363.
86. S. Das Gupta and A.Z. Mekjian, to be published in Phys. Reports.
87. H.H. Gutbrod, A. Sandoval, P.J. Johansen, A.M. Poskanzer, J. Gosset, W.G. Meyer, G.D. Westfall and R. Stock, Phys. Rev. Lett. 37 (1976) 667.
88. A. Mekjian, Phys. Rev. Lett. 38 (1977) 640; Phys. Rev. C17 (1978) 1051; Phys. Lett. 89B (1980) 177.
89. M.C. Lemaire, S. Nagamiya, S. Schnetzer, H. Steiner and I. Tanihata, Phys. Lett. 85B (1979) 38.
90. G. Gaul, R. Glasow, H. Lohner, B. Ludewigt and R. Santo, private communication.
91. M.C. Lemaire, S. Nagamiya, S. Schnetzer, H. Steiner and I. Tanihata, Contribution to this Conference, p 614.
92. S.Y. Fung, W. Gorn, G.P. Kiernan, J.J. Lu, Y.T. Oh and R.T. Poe, Phys. Rev. Lett. 41 (1978) 1592.
93. J. Bartke, Contribution to this Conference, p. 537.
94. A. Sagle, F. Zarbakhsh, J. Carroll, V. Perez-Mendez, T. Mulera, I. Tanihata, G. Igo and J. Oostens, Contribution to this Conference, p. 510.

95. H. Machner, Phys. Rev. C21 (1980) 2695; Phys. Lett 86B (1979) 129; contribution to this Conference, p 403.
96. S. Nagamiya, K. Anderson, W. Bruckner, O. Chamberlain, M.C. Lemaire, S. Schnetzer, G. Shapiro, H. Steiner and I. Tanihata, Phys. Lett. 81B (1979) 147.
97. H.C. Chiang and J. Hufner, University of Heidelberg, Preprint, 1980.
98. P.J. Siemens, Proc. of INS Kukuchi School on Nucl. Phys. at High Energies, Fuji-Yoshida, Japan, 1980.
99. Y. Chu, P. Doll, A. Gobbi, K. Hildenbrand, H. Ho, W. Kuhn, H. Lohner, U. Lynen, W. Muller, A. Olmi, D. Pelte, H. Sann, R. Santo and U. Winkler, Contribution to this Conference, p. 557.
100. W.G. Meyer, H.H. Gutbrod, Ch. Lukner and A. Sandoval, Phys. Rev. C22 (1980) 179.
101. J.P. Bondorf, Proc. of Conf. on Large Amplitude Collective Nuclear Motion, Lake Balaton 1979, p. 482.
102. R. Kullberg and Oskarsson, Z. Phys. A288 (1978) 283.
103. I. Otterlund, Talk presented at Symposium on Intermediate Energy Heavy Ion Collisions, Copenhagen, 1979.
104. H. Stocker and B. Muller, GSI Preprint 80-4 (1980).
105. R. Stock, H.H. Gutbrod, W.G. Meyer, A.M. Poskanzer, A. Sandoval, J. Gosset, Ch. King, G. King, Ch. Lukner, N. Vansen, G.D. Westfall and K. Wolf, Phys. Rev. Lett. 44 (1980) 1243.
106. For further discussion of concepts relevant to this paper see: Proc. Symp. on Heavy-Ion Physics from 10 to 200 MeV/u, Brookhaven, 1979, BNL Report 51115; Proc. of Summer School on Physique Des Ions Lourds de 30 MeV par Nucleon, Serre-Chevalier, 1979, ISN Grenoble Report, ed. by N. Longequeue; D.K. Scott, Prog. Nucl. and Part. Phys. 4 (1980) 5, and Theoretical methods in Medium and Heavy Ion Physics ed. K. McVoy and W.A. Friedman (Plenum) p. 3; Proc. of Int. Conf. on Extreme States in Nuclear Systems, Dresden 1980, to be published; see also Ref. 53.